Inorg. Chem. **2007**, *46*, 299–308

Syntheses, Structures, Spectroscopy, and Chromotropism of New Complexes Arising from the Reaction of Nickel(II) Nitrate with Diphenyl(dipyrazolyl)methane

Natalie Baho and Davit Zargarian*

Département de Chimie, Université de Montréal, C. P. 6128, Succursale Centre-ville, Montréal, Québec, Canada H3C 3J7

Received July 14, 2006

The complexes [(dpdpm)Ni(η^2-NO_3)$_2$] (**1**), [(dpdpm)Ni(η^2-NO_3)(η^1-NO_3)(CH_3CN)] (**2**), [(dpdpm)$_2$Ni(η^1-NO_3)(H_2O)]-NO_3 (**3**), and [(dpdpm)$_2$Ni(H_2O)$_2$][NO_3]$_2$ (**4**) (dpdpm = diphenyl(dipyrazolyl)methane, $Ph_2C(C_3N_2H_3)_2$), have been prepared and characterized by IR and UV–vis–NIR spectroscopy and X-ray diffraction studies. X-ray studies have confirmed that complexes **1**–**4** all adopt variously distorted octahedral structures in the solid state, the largest distortions arising from the small bite-angle of the bidentate nitrate ligand in **1** and **2**. Magnetic moment measurements indicate that these solids are paramagnetic with two unpaired electrons. The solution ^{1}H NMR data show that the paramagnetism is maintained in solution. Absorption spectra of **1**–**4** show three main bands in the region of 350–1000 nm representing spin allowed (d–d) transitions from the ground state $^3A_{2g}$ to the excited states $^3T_{2g}$, $^3T_{1g}(^3F)$, and $^3T_{1g}(^3P)$. A weak shoulder was also detected at about 700–800 nm in most spectra, representing spin-forbidden transitions $^3A_{2g} \rightarrow {}^1Eg$. A comparison of the crystal field parameters 10Dq and B for **1**–**4** to the corresponding values for related complexes indicated that these parameters are fairly insensitive to structural variations within this family of complexes. The 10Dq/B ratios show greater variations, but no clear correlations are apparent between 10Dq/B and such structural features as the nature of ligator atoms (N:O ratio), the bonding mode of the nitrate ligand, or the overall charge. Complexes **1** (green) and **2** (blue) interconvert as a function of temperature (solutions and solid samples), concentration of CH_3CN (solutions), or CH_3CN vapor pressure (solid samples).

Introduction

Since Trofimenko's initial reports on poly(pyrazolyl)-borates[1] and poly(pyrazolyl)alkanes,[2] these so-called scorpionate ligands have found wide applications in coordination, organometallic, and bioinorganic chemistry.[3] Perhaps the most important feature of these two classes of ligands is the ease with which their steric and electronic properties can be modified by simple synthetic modifications, thereby allowing a fine-tuning of ligand properties. The anionic bis- or tris-(pyrazolyl)borates are the most commonly studied of the scorpionate ligands. This family of ligands has shown great versatility for stabilizing a wide range of coordination and organometallic complexes, in particular those possessing metals in their less common oxidation states (e.g., Pd(IV)[4,5] and Pt(IV)[6]). By comparison, the neutral bis- or tris-(pyrazolyl)alkanes have had less impact in organometallic chemistry.[7] The paucity of organometallic compounds based on poly(pyrazolyl)alkane ligands is particularly evident in

* To whom correspondence should be addressed. Phone: 514-343-2247. Fax: 514-343-2468. E-mail: zargarian.davit@umontreal.ca.

(1) (a) Trofimenko, S. *J. Am. Chem. Soc.* **1966**, *88*, 1842. (b) Trofimenko, S. *J. Am. Chem. Soc.* **1967**, *89*, 3170. (c) Trofimenko, S. *J. Am. Chem. Soc.* **1967**, *89*, 6288. (d) Trofimenko, S. *J. Am. Chem. Soc.* **1969**, *91*, 588. (e) Trofimenko, S. *J. Am. Chem. Soc.* **1970**, *92*, 5118.

(2) Trofimenko, S. *J. Am. Chem.* Soc. **1970**, *92*, 1499.

(3) For a few recent reviews on the development of the coordination chemistry of scorpionate ligands, see: (a) Reger, D. L. *Comments Inorg. Chem.* **1999**, *21*, 1. (b) Sadimenko, A. P. *Adv. Heterocycl. Chem.* **2001**, *81*, 167. (c) Trofimenko, S. *Chem. Rev.* **1993**, *93*, 943. (d) Trofimenko, S. *Polyhedron* **2004**, *23*, 197. (e) Otero, A; Fernàndez-Baeza, J.; Antiñolo, A.; Tejeda, J.; Lara-Sanchez, A. *Dalton Trans.* **2004**, 1499. (f) Pettinari, C.; Pettinari, R. *Coord. Chem. Rev.* **2005**, *249*, 525. (g) Pettinari, C.; Pettinari, R. *Coord. Chem. Rev.* **2005**, *249*, 663. (h) Bigmore, H. R.; Lawrence, S. C.; Mountford, P.; Tredget, C. S. *Dalton Trans.* **2005**, 635.

(4) Byers, P. K.; Canty, A. J.; Honeyman, R. T. *Adv. Organomet. Chem.* **1992**, *34*, 1. (See in particular pp. 26 and 34.)

(5) Canty, A. J.; Andrew, S.; Skelton, B. W.; Traill, P. R.; White, A. H. *Organometallics* **1995**, *14*, 199.

(6) Reinartz, S.; Brookhart, M.; Templeton, J. L. *Organometallics* **2002**, *21*, 247.

(7) Byers, P. K.; Canty, A. J.; Skelton, B. W.; White, A. H. *Organometallics* **1990**, *9*, 826.

10.1021/ic061311z CCC: $37.00 © 2007 American Chemical Society
Published on Web 12/07/2006

the case of nickel, for which no organometallic complex has been reported.[8]

We have explored the preparation and characterization of new nickel−poly(pyrazolyl)alkane complexes as precursors for new organometallic species.[9] In previous reports we have described the synthesis,[10] structural characterization,[11] and spectroscopy[12] of a series of complexes based on bpm* and tpm* ligands (bpm* = bis(3,5-dimethylpyrazolyl)methane, tpm* = tris(3,5-dimethylpyrazolyl)methane). All of these compounds are paramagnetic and some display continuous thermo-, solvato-, and vapochromic behavior. These properties arise from the relatively facile changes in the coordination geometry of these compounds or from the substitution of one or more ligands by solvent molecules or coordinating anions. The observation of these phenomena in our complexes implies the existence of closely related structural derivatives of very comparable energies.

Thermochromic behavior has been observed with other Ni(II) complexes bearing bis(pyrazolyl)methane or ethylenediamine type ligands. For instance, dichloro(bis(3,5-dimethylpyrazolyl)methane)Ni^{II} undergoes a monomer−dimer equilibrium (in the solid state) as a function of temperature: the orange, chloro-bridged dimer is stable below 130 °C and adopts a square pyramidal geometry, while the deep purple monomer forms at higher temperatures and adopts a pseudo-tetrahedral geometry around Ni.[1e,13] On the other hand, the complex [bis(*N*,*N*-diethylethylenediamine)-Ni^{II}][NO_3]$_2$ and its Cu^{II} analogue undergo reversible coordination of the nitrate anions to convert the red square planar form to a purple octahedral species at high temperatures.[13,14]

Solvatochromism of Ni(II) species based on ethylenediamine type ligands has been studied intensively.[15] These studies have shown that the solvatochromism of these complexes is based, primarily, on the coordination of solvent molecules to the metal center in the initially square planar species; depending on the donor strength of the solvent or the steric bulk of the ligands, one or two solvent molecules can bind to give square pyramidal or octahedral solvato products, respectively. In some cases, the coordinating ability of certain anions can modulate the outcome of these interactions. Similarly, vapochromism arises from metal−ligand or metal−metal interactions, or more subtle changes in the compound lattice, when a complex is exposed to volatile organic compounds; this phenomenon leads to changes in the absorption or luminescence properties of the complex. Vapochromism has been studied extensively with a number of transition metal compounds, including those of platinum[16] and gold,[17] but very few studies have been reported with Ni(II) complexes. For instance, a recent report outlined the development of sensors based on the vapochromic properties of the complex bis(1,2,6,7-tetracyano-3,5-dihydro-3,5-diiminopyrrolizinido)nickel(II) dispersed inside spin coated poly(vinylbutyral) thin films.[18] To our knowledge, the vapochromic properties of Ni complexes based on bis(pyrazolyl)methane type ligands have not been explored.

As a follow-up to our earlier studies, we have prepared a new series of nickel complexes featuring the ligand dpdpm (dpdpm = diphenyl(dipyrazolylmethane)).[19] Solid state structural studies and UV−vis−NIR spectroscopy have been employed to investigate structural changes in the first examples of this family of compounds as a function of temperature, different solvents, and type of anions used. Herein we report on the synthesis, structural characterization, and spectroscopy of complexes arising from the reaction of dpdpm with $Ni(NO_3)_2$. The relatively labile coordination of the nitrate anion has given access to compounds featuring η^2-, η^1-, and η^0-nitrate moieties. Thus, the nitrate ligand in the complex [(dpdpm)Ni(η^2-NO_3)$_2$], **1**, undergoes a hapticity change to give [(dpdpm)Ni(η^1-NO_3)(η^2-NO_3)(CH_3CN)], **2**; these two compounds interconvert as a function of temperature (solutions and solid samples), acetonitrile concentration (solutions), or acetonitrile vapor pressure (solid samples).

Experimental Section

General Procedure. All starting materials were purchased from Sigma-Aldrich and used as received. $Ni(NO_3)_2$·H_2O was used without dehydration. The main ligand used in this study, diphenyl-(dipyrazolyl)methane (dpdpm), was synthesized according to a published procedure.[19b] The NMR spectra were recorded on a

(8) For recent reports on organometallic complexes of Pd based on poly(pyrazolyl)alkane ligands, see: (a) Sánchez, G.; Serrano, L. J.; Pérez, J.; Ramirez de Arellano, M. C.; López, G.; Molins, E. *Inorg. Chem. Acta* **1999**, *295*, 136. (b) Jalón, A. F.; Arroyo, N.; Gómez-de La Tore, F.; Manzano, B. R.; Moreno-Lara. B.; Rodriguez., A. M. *J. Organomet. Chem.* **2000**, *603*, 174. (c) Tsuji, S.; Swenson, D. C.; Jordan, R. F. *Organometallics* **1999**, *18*, 4758.

(9) For representative reports on coordination complexes of Ni featuring poly(pyrazolyl)alkane ligands, see: (a) Mahon, M. F.; McGinley, J.; Molloy, K. C. *Inorg. Chim. Acta* **2003**, *355*, 368. (b) Wolfgang, K.; Berghahn, M.; Frank, W.; Reiss, G. J.; Schonherr, T.; Rheinwald, G.; Lang, H. *Eur. J. Inorg. Chem.* **2003**, *11*, 2059. (c) Pettinari, C.; Marchetti, F.; Cingolani, A.; Leonesi, D.; Colapietro, M.; Margadonna, S. *Polyhedron* **1998**, *17*, 4145. (d) Mann, K. L.; Jeffery, J. C.; McCleverty, J. A.; Thornton, P.; Ward, M. D. *J. Chem. Soc., Dalton Trans.* **1998**, *1*, 89. (e) Pettinari, C.; Cingolani, A.; Bovio, B. *Polyhedron* **1996**, *15*, 115. (f) Astley, T.; Gulbis, J. M.; Hitchman M. A.; Tiekink, E. R. T. *J. Chem. Soc., Dalton Trans.* **1993**, 509. (g) Mesubi, M. A.; Omotowa, B. A. *Synth. React. Inorg. Met.-Org. Chem.* **1993**, *23*, 213. (h) Astley, T.; Canty, A. J.; Hitchman, M. A.; Rowbottom, G. L.; Skelton, B. W.; White, A. H. *J. Chem. Soc., Dalton Trans.* **1991**, 1981. (i) Reedijk, J.; Verbiest, J. *Transition Met. Chem.* **1979**, *4*, 239. (j) Jansen, J. C.; Van Koningsveld, H.; Van Ooijen, J. A. C.; Reedijk, J. *Inorg. Chem.* **1980**, *19*, 170. (k) Reedijk, J.; Verbiest, J.; *Transition Met. Chem.* **1978**, *3*, 51.

(10) Michaud, A.; Fontaine, F.-G.; Zargarian, D. *Inorg. Chim. Acta* **2006**, *359*, 2592.

(11) (a) Michaud, A.; Fontaine, F.-G.; Zargarian, D. *Acta Crystallogr.* **2005**, E *61*, m784. (b) Michaud, A.; Fontaine, F.-G.; Zargarian, D. *Acta Crystallogr.* **2005**, E *61*, m904.

(12) Nolet, M.-C.; Michaud, A.; Bain, C.; Zargarian, D.; Reber, C. *Photochem. Photobiol.* **2006**, *82*, 57.

(13) Bloomquist, D. R.; Willett, R. D. *Coord. Chem. Rev.* **1982**, *47*, 125.

(14) Fabbrizzi, L.; Micheloni, M.; Paoletti, P. *Inorg. Chem.* **1974**, *13*, 3019.

(15) (a) Fukuda, Y.; Cho, M.; Sone, K. *Bull. Chem. Soc. Jpn.* **1989**, *62*, 51. (b) Bourdin, D.; Lavabre, D.; Beteille, J. P.; Levy, G.; Micheau, J. *Bull. Chem. Soc. Jpn.* **1990**, *63*, 2985. (c) Linert, W.; Gutmann, V. *Coord. Chem. Rev.* **1992**, *117*, 159. (d) Linert, W.; Fukuda, Y.; Camard, A. *Coord. Chem. Rev.* **2001**, *218*, 113. (e) Berger, S. *Z. Phys. Chem.* **2002**, *216*, 1363.

(16) Wadas, T. J.; Wang, Q. M.; Kim, Y. J.; Fraschenreim, C.; Blanton, T. N.; Eisenberg, T. *J. Am. Chem. Soc.* **2004**, *126*, 16841.

(17) Lefebvre, J.; Batchelor, R. J.; Leznoff, D. B. *J. Am. Chem. Soc.* **2004**, *126*, 16117.

(18) Flamini, A.; Mattei, G.; Panusa, A. *J. Inclusion Phenom.* **2004**, *33*, 377.

(19) Recent reports have described a number of dpdpm complexes of copper (a) and silver (b): (a) Shaw, J. L.; Cardon, T. B.; Lorigan, G. A.; Ziegler, C. J. *Eur. J. Inorg. Chem.* **2004**, 1073. (b) Reger, D. L.; Gardinier, J. R.; Smith, M.D. *Inorg. Chem.* **2004**, *43*, 3825.

Bruker Av400 (^{1}H at 400 MHz). The IR spectra were recorded between 4000 and 400 cm^{-1} using KBr pellets on a Perkin-Elmer Spectrum One spectrophotometer using the Spectrum v.3.01.00 software. The UV−vis−NIR spectra were recorded between 1300 and 250 nm with a 1 cm quartz cell on a Varian Cary 500i; baseline correction was applied prior to recording the spectra. The magnetic susceptibility measurements were carried out at room temperature using the Gouy method with a Johnson Matthey Magnetic Susceptibility Balance calibrated on [$HgCo(SCN)_4$] samples. The elemental analyses (C, H, and N) were performed in duplicate by Laboratoire d'Analyse Élémentaire de l'Université de Montréal.

Syntheses. [(dpdpm)Ni(η^2-NO_3)$_2$] (1). Solid $Ni(NO_3)_2 \cdot H_2O$ (0.45 g, 1.67 mmol) was added to a stirred solution of dpdpm (0.50 g, 1.67 mmol) in CH_2Cl_2 (40 mL), and the reaction mixture was heated to reflux for 4 h. The final mixture was cooled to room temperature, filtered, and evaporated to give a dark turquoise-green solid. This was washed with hot hexane (2 × 40 mL) and extracted into CH_2Cl_2 to remove insoluble impurities. Removal of the solvent gave a turquoise-green solid (0.67 g, 83% yield). X-ray quality single crystals (emerald green) were obtained by diffusion of Et_2O into a concentrated CH_2Cl_2 solution. ^{1}H NMR ($CDCl_3$): δ 62.05 (br), 44.43 (br), 7.21 (br), 6.87 (br). IR (KBr): ν (cm^{-1}) 3429.62 (br), 3137.69 (m), 2506 (w), 1768.79 (m), 1522 (s), 1491 (vs), 1452 (s), 1434 (s), 1408 (s), 1384 (s), 1308 (s), 1278 (s), 1260(m), 1217 (w), 1194 (w), 1165(w), 1102 (s), 1087 (w), 1068 (s), 1016 (m), 1001 (w), 958 (w), 940 (w), 921 (w), 891 (w), 861 (w), 807 (w), 785 (m), 750 (s), 699 (s), 659 (s), 636 (w), 604 (w). mp: 240 °C. $\mu_{eff.}$: 3.22 BM. Anal. Calcd for $C_{19}H_{16}N_6O_6Ni$: C, 47.24; H, 3.34; N, 17.40. Found: C, 47.28; H, 3.40; N, 17.00.

[(dpdpm)Ni(η^1-NO_3)(CH_3CN)][NO_3] (2). To a solid sample of complex **1** (0.4 g, 0.828 mmol) was added a sufficiently small amount of CH_3CN (0.55 g, 13 mmol) to avoid complete dissolution of the solid. The color of the "wet" solid changed immediately from green to blue. Placing the "wet" blue solid and the residual blue solution under vacuum for a brief period (1−2 min) gave a blue solid (0.34 g, 78% yield). X-ray quality crystals (blue) of the new product were grown by diffusion of Et_2O into a saturated CH_3CN solution. ^{1}H NMR (CD_3CN): δ 67.7 (br), 65.8 (br), 54.0 (br), 44.4 (br), 7.32 (br), 7.03 (br), 2.11 (br). (NB: The spectra of aged solutions also displayed broadened signals for free dppm, and the broad signal at 2.11 merged with the residual solvent peak.) IR (KBr): ν (cm^{-1}) 3401 (br), 3151 (m), 3064 (m), (w), 2314 (w), 2288 (w), (w), 1619 (m), 1492 (vs), 1450 (vs), 1435 (s), 1407(s), 1384(s), 1306 (vs), 1277(s), 1220 (m), 1194 (m), 1171(w), 1105 (m), 1085 (w), 1069 (s), (w), 1018 (w), 1000 (m) 939 (m), 921 (m), 890 (m), 871 (m), 808 (m), (s), 752 (vs), 698 (s), 658 (m), 636 (m), 605 (w). μ_{eff}:. 3.86 BM. mp: 238 °C. The elemental analysis of this compound was problematic because thorough evaporation of the sample resulted in an analysis identical to that of complex **1** (i.e., loss of coordinated CH_3CN). To minimize the loss of CH_3CN, a batch of crystals was heated *for a few seconds only* in a 100 °C oven prior to the analysis, which gave results consistent with the inclusion of one-half molecule of Et_2O: Found: C, 49.16; H, 3.98; N, 17.53. (Calcd for $C_{21}H_{19}N_7O_6Ni$: C, 48.12; H, 3.65; N, 18.71. Calcd for $C_{21}H_{19}N_7O_6Ni + {}^1/_2(C_4H_{10}O)$: C, 49.23; H, 4.31; N, 17.47.)

[(dpdpm)$_2$Ni(H_2O)(η^1-NO_3)][NO_3] (3). Solid $Ni(NO_3)_2 \cdot H_2O$ (0.24 g, 0.83 mmol) was added to a stirred solution of dpdpm (0.50 g, 1.67 mmol) in CH_2Cl_2 (40 mL), and the reaction mixture was heated to reflux for 4 h. The final mixture was cooled to room temperature, filtered, and evaporated to give a royal blue solid. This was washed with hot hexane (2 × 40 mL) and extracted into CH_2Cl_2 to remove insoluble impurities. Removal of the solvent gave a royal blue solid (0.60 g, 91% yield). X-ray quality single crystals (navy blue) were obtained by diffusion of Et_2O into a concentrated CH_2Cl_2 solution. ^{1}H NMR ($CDCl_3$): δ 68.4 (br), 62.4 (br), 44.0 (br), 37.5 (br), 8.0−7.0 (br), 6.9 (br), plus sharp signals due to free dpdpm at 7.69 (s), 7.55 (d, J = 3), 7.37 (psq, J = 8), 7.07 (d, J = 8), 6.30 (s). IR (KBr): ν (cm^{-1}) 3402 (br), 3135 (w), 3121 (m), 3059 (m), 3035 (m), 2926 (w), 2854 (w), 2427 (w), 1996 (w), 1748 (w), 1631 (m), 1517 (m), 1493 (m), 1448−1438 (s), 1384 (s), 1339 (m), 1326 (m), 1305−1293 (w), 1249 (w), 1219 (m), 1195 (m), 1168 (m), 1112 (s), 1087 (m), 1066 (s), 1038 (w), 1001(w), 991 (w), 939 (w), 921 (w), 891 (w), 873 (w), 863 (w), 826 (w), 757−748 (vs), 700 (vs), 659 (w), 638 (m), 618 (w), 607 (w), 511 (w). μ_{eff}: 3.36 BM. mp: 145 °C. Anal. Calcd for $C_{38}H_{34}N_{10}O_7Ni$: C, 56.95; H, 4.28; N, 17.48. Found: C, 56.54; H, 4.26; N, 17.42.

[(dpdpm)$_2$Ni (H_2O)$_2$][NO_3]$_2$ (4). Solid $Ni(NO_3)_2 \cdot 6H_2O$ (0.24 g, 0.83 mmol) was added to a stirred solution of dpdpm (0.50 g, 1.67 mmol) in MeOH (40 mL), and the reaction mixture was refluxed for 18 h. The final mixture was cooled to room temperature, filtered, and evaporated to give a dark blue solid. This was washed with hot hexane (3 × 50 mL) and extracted into CH_2Cl_2 to remove insoluble impurities. Removal of the solvent gave a dark blue solid (0.56 g, 82% yield). X-ray quality single crystals (blue) were obtained by diffusion of Et_2O into a concentrated MeOH solution. ^{1}H NMR ($CDCl_3$): δ 65.7 (br), 52.7 (br), 45.3 (br), 49.0 (br), 7.7−6.5 (br), plus signals corresponding to free dpdpm. IR (KBr): ν (cm$^{-1)}$ 3390 (br), 3164 (m), 3130 (m), 33120 (m), 3056 (m), 2418 (w), 1655 (m), 1518 (m), 1492 (m), 1449−1385 (vs), 1332−1306 (vs), 1251(m), 1219 (m), 1189 (s), 1165 (m), 1109 (m), 1086 (m), 1063 (s), 1041 (m), 994 (w), 982 (w), 938 (w), 915 (w), 890 (w), 872 (w), 823 (w), 753 (vs), 698 (vs), 659 (w), 635 (m), 605 (w), 501 (w). μ_{eff}: 3.17 BM. mp: 195−205 °C. Anal. Calcd for $C_{38}H_{36}N_{10}O_8Ni$: C, 55.70; H, 4.43; N, 17.09. Found: C, 55.25; H, 4.35; N, 17.03.

Crystallographic Studies. The crystal data for compound **1** were collected on an Enraf-Nonius CAD4 four-cycle goniometer at 298-(2) K. The diffraction data were collected with graphite-monochromated Cu Kα radiation; the cell parameters were refined using CAD-4 software on 25 reflections, while NRC-2 and NRC-2A were used for the data reduction.[20] The crystal data for **2**, **3**, and **4** were collected on a Bruker AXS SMART 6K diffractometer mounted with rotating anode Cu Kα radiation at 293(2) K (SMART[21] software). Cell refinement and data reduction were carried out using SAINT.[22] All structures were solved by direct methods using SHELXS97,[23] and the refinements were done on F^2 by full-matrix

(20) (a) Ahmed, F. R.; Hall, S. R.; Pippy, M. E.; Huber, C. P. NRC Crystallographic Computer Programs for the IBM/360. Accession Nos. 133−147. In *J. Appl. Crystallogr.* **1973**, *6*, 309. (b) Bruker (1997). SHELXTL (1997). Release 5.10. The Complete Software Package for Single Crystal Structure Determination. Bruker AXS Inc., Madison, WI. (c) Enraf-Nonius (1989). CAD-4 Software. Version 5. Enraf-Nonius, Delft, The Netherlands. (d) LePage, Y. *J. Appl. Crystallogr.* **1987**, *20*, 264−269. (e) Nonius (1998). Collect Software. Nonius B.V., Delft, The Netherlands. (f) Sheldrick, G. M. (1986). SHELXS86. Program for Crystal Structure solution. University of Gottingen, Germany. (g) Sheldrick, G. M. (1997a). SHELXS97. Program for Crystal Structure solution. University of Gottingen, Germany. (h) Sheldrick, G. M. (1997b). SHELXL97. Program for crystal structure refinement. University of Gottingen, Germany. (i) Spek, A. L. (2000). PLATON, 2000 version. Molecular Geometry Program. University of Utrecht, Utrecht, Holland. (j) Gabe, E. J.; Le Page, Y.; Charlant, J. P.; Lee, F. L.; White, P. S. *J. Appl. Crystallogr.* **1989**, *22*, 384.
(21) SMART (2001). Release 5.059. Bruker Molecular Analysis Research Tool. Bruker AXS Inc., Madison, WI.
(22) SAINT (2003). Release 6.06. Integration Software for Single Crystal Data. Bruker AXS Inc., Madison, WI.
(23) Sheldrick, G. M. SHELXS, Program for the Solution of Crystal Structures. University of Goettingen, Germany, 1997.

Table 1. Crystallographic Data for Complexes **1**−**4**

	1	**2**·0.5Et_2O	3	4
formula	$C_{19}H_{16}N_6O_6Ni$	$C_{21}H_{19}N_7O_6Ni$·0.5$C_4H_{10}O$	$C_{38}H_{34}N_{10}O_7Ni$	$C_{38}H_{36}N_{10}O_8N$ i
mol wt	483.09	561.20	801.46	819.48
cryst color	green	blue	blue	blue
cryst dimens, mm	0.26 × 0.15 × 0.14	0.24 × 0.26 × 0.3	0.33 × 0.26 × 0.13	0.16 × 0.14 × 0.12
symmetry	monoclinic	triclinic	monoclinic	monoclinic
space group	*P*21/*n*	$P\bar{1}$	*P*21/*c*	*P*21/*c*
a, Å	8.400(2)	8.4150(2)	13.5458(8)	11.6537(2)
b, Å	14.861(5)	9.4669(2)	16.9361(9)	16.4081(3)
c, Å	17.029(6)	16.6064(3)	16.4455(9)	19.2521(3)
α, deg	90	76.1910(10)	90	90
β, deg	102.17(2)	85.0970(10)	104.175(3)	92.0130(10)
γ, deg	90	86.125(2)	90	90
volume, $Å^3$	2078.0(11)	1278.47(5)	3657.9(4)	3679.02(11)
Z	4	2	4	4
D(calcd), g cm^{-1}	1.544	1.458	1.455	1.479
diffractometer	CAD-4	Bruker AXS SMART 2K	Bruker AXS SMART 2K	Bruker AXS SMART 2K
temp, K	293(2)	200(2)	220(2)	200(2)
l	1.5418	1.5418	1.5418	1.5418
μ, mm^{-1}	1.798	1.569	1.318	1.344
scan type	*ω* scan	*ω* scan	*ω* scan	*ω* scan
F(000)	992	582	1664	1704
θ_{max}, (deg)	69.92	73.01	72.03	68.89
h, *k*, *l* range	$-10 \le h \le 10$ $-18 \le k \le 18$ $-20 \le l \le 20$	$-10 \le h \le 10$ $-11 \le k \le 11$ $-20 \le l \le 20$	$-16 \le h \le 15$ $-20 \le k \le 20$ $-19 \le l \le 20$	$-14 \le h \le 13$ $-18 \le k \le 19$ $-23 \le l \le 23$
reflns obsvd ($I > 2\sigma(I)$)	3382	6433	6504	5518
absorption correction	multiscan SADABS	multiscan SADABS	multiscan SADABS	multiscan SADABS
T (min, max)	0.65, 0.79	0.76, 0.65	0.94,0.70	0.80, 0.85
R [$F^2 > 2\sigma(F^2)$], *wR*(F^2)	0.0444, 0.1143	0.0525, 0.1296	0.0506, 0.1238	0.0325, 0.0924
GOF	1.042	1.041	1.052	1.036

least-squares.[24] All non-hydrogen atoms were refined anisotropically. The positional parameters for H atoms in water molecules were refined isotropically, but all other hydrogens were constrained to the parent atom using a riding model.

The monodentate nitrate ligand of complex **2** showed some disorder in the positions of the O5 and O55 atoms; the occupancies of these atoms were initially refined and then fixed at 0.50. This structure also contained disordered Et_2O molecules, which were refined isotropically using a constrained model; disordered solvent molecules were then introduced over two positions and refined using ISOR restrained technique. The crystal structures of **3** and **4** are stabilized by intermolecular hydrogen bonds. The details on O−H···O distances are available from the detailed structure reports (Supporting Information). For the sake of clarity, the disordered Et_2O molecules in **2** and the counter ions in **3** and **4** have been removed from the ORTEP diagrams. All the details concerning the refinement of the crystal structures are listed in Table 1.

Testing the Reversible Chromotropic Properties of Complexes 1 and 2. A. Solvatochromic Behavior of Complexes 1 and 2. Dissolving ca. 15 mg of green complex **1** in ca. 1 mL of CH_2Cl_2 gave a green solution. Evaporating this solution to dryness gave back the green solid, which was dissolved in ca. 1 mL of CH_3CN to give a blue solution. Evaporation of CH_3CN to dryness gave back the original green solid. Redissolving the green solid in CH_3CN followed by evaporation resulted in the same color changes.

In order to confirm that the observed color changes correspond to the interconversion of complexes **1** and **2**, UV−vis−NIR spectra were recorded for samples of **1** in CH_2Cl_2 and CH_3CN. The spectrum of the CH_3CN solution of **1** was identical to that of complex **2** in CH_3CN. UV−vis−NIR spectra were also recorded for CH_2Cl_2:CH_3CN mixtures of various proportions (ca. 6.5 mM). The narrowest absorptions in the spectra obtained for 100:0 and 0:100 samples (at 381 and 374 nm, respectively) were selected for monitoring the solvent-induced interconversion of the two complexes. The spectra for the 80:20, 60:40, 50:50, 40:60, and 20:80 samples showed an incremental shift in the peak maximum, as shown in Figure 7.

B. Reversible Vapochromic Behavior of Complexes 1 and 2. A small, uncapped vial containing 4 mg of complex **1** was placed inside a 25 mL round-bottom flask containing ca. 3 mL of CH_3CN; care was taken to make sure that the solid and the solvent did not come in direct contact. The flask was then stoppered to allow a build-up of solvent vapor at room temperature. The turquoise-green color of complex **1** changed to light blue in 8 min. At this point, the sample vial was taken out of the flask and placed in a 100 °C oven for 1 min, which caused the original turquoise-green color of the sample to reappear; the sample did not show any visible sign of degradation. Exposing the green solid to CH_3CN vapors resulted once again in a green-to-blue color change. Repeating this procedure five times on the same sample showed the same observations: samples of **1** obtained by heating **2** for only 1 min at 100 °C required between 5 and 10 min (the average over five trials being 7 min) of exposure to CH_3CN vapors to undergo the green-to-blue color change in a convincing fashion.

C. Reversible Thermochromic Behavior of Complexes 1 and 2. Dissolving a solid sample of turquoise-green **1** in CH_3CN (ca. 0.02 M) gave a blue solution at ambient temperature. Heating this solution to 65 °C resulted in a rapid color change to the green color of CH_2Cl_2 solutions of **1**. This color could be maintained over 45 min of heating without decomposition. Cooling the green solution to 18 °C regenerated the initial blue color of the sample. Repeating

(24) (a) Bruker (1997). SHELXTL (1997). Release 5.10. The Complete Software Package for Single Crystal Structure Determination. Bruker AXS Inc., Madison, WI. (b) Bruker (1999a). SAINT (2003). Release 7.06. Integration Software for Single Crystal Data. Bruker AXS Inc., Madison, WI. (c) Bruker (1999b). SMART (2001). Release 5.625. Bruker Molecular Analysis Research Tool. Bruker AXS Inc., Madison, WI. (d) Sheldrick, G. M. (1996). SADABS, Bruker Area Detector Absorption Corrections. (e) Bruker AXS Inc., Madison, WI.

Scheme 1

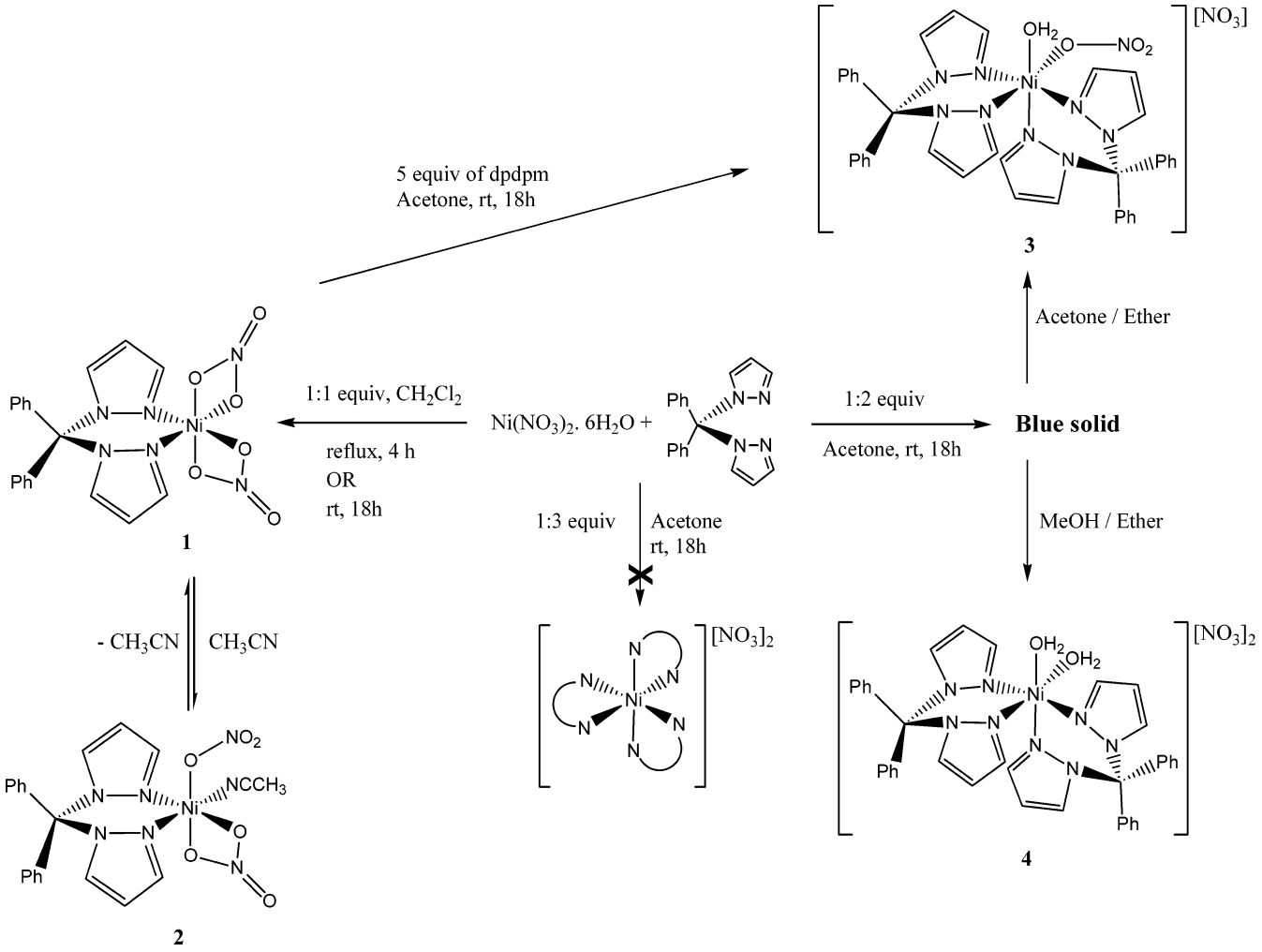

this heating−cooling cycle 10 times confirmed the reversible nature of this thermochromic behavior. Evaporation of the solution furnished the green complex **1** unchanged.

In a similar experiment, we recorded the variable temperature (264−360 K) UV−vis−NIR spectra of a solution of **1** in CH_3CN, and the thermochromic behavior was monitored by following the high-energy absorption peaks (ca. 370−380 nm). This experiment showed that higher temperatures result in an incremental shift in the band maximum of the monitored absorption, from ca. 370 nm (for **2**) to ca. 380 nm (for **1**).

Results and Discussion

Syntheses. The reaction of $Ni(NO_3)_2 \cdot H_2O$ with 1 equiv of dpdpm in CH_2Cl_2 under reflux over 4 h afforded a green solution, which was evaporated to give complex **1** as a turquoise-green solid (Scheme 1). The same result can be obtained from the room temperature reaction during 18 h. Washing the turquoise-green solid with hot hexane to remove any excess of unreacted ligand, followed by extraction into CH_2Cl_2 to eliminate unreacted $Ni(NO_3)_2 \cdot 6H_2O$, yielded an analytically pure product. Recrystallization from CH_2Cl_2/Et_2O gave emerald green crystals that were subjected to spectral analysis and X-ray diffraction studies (vide infra). Bis(η^2-NO_3) complexes of Ni similar to **1** have been reported.[25]

The analogous reaction of $Ni(NO_3)_2 \cdot 6H_2O$ with 2 equiv of dpdpm gave, after workup and purification, a blue solid. Contrary to our expectations, this product was neither $[(dpdpm)_2Ni(\eta^2\text{-}NO_3)][NO_3]$ nor $[(dpdpm)_2Ni(\eta^1\text{-}NO_3)_2]$. Indeed, the final outcome of the reaction depended on the solvent of recrystallization, producing $[(dpdpm)_2Ni(\eta^1\text{-}NO_3)(H_2O)]$, **3**, from acetone, or $[(dpdpm)_2Ni(H_2O)_2]$, **4**, from CH_2Cl_2, CH_3CN, or MeOH. Complexes **3** and **4** were studied by spectroscopy and X-ray diffraction studies (vide infra).

The formation of **3** and **4** indicates that the nitrate ligand in these bis(dpdpm) species is very labile and can be displaced readily by residual water. In an effort to prevent the displacement of the nitrate ligands by water, the reaction of $Ni(NO_3)_2$ with 2 equiv of dpdpm was carried out in dry CH_2Cl_2 under an atmosphere of dry nitrogen. This reaction gave a lilac solid that proved to be very sensitive to water: exposure of this new product to air for a few minutes converted it to complex **3**. We were unable to identify the lilac solid, but its facile hydration to **3** suggests it might be one of the anticipated precursors to **3**, i.e., $[(dpdpm)_2Ni(\eta^2\text{-}NO_3)][NO_3]$ or $[(dpdpm)_2Ni(\eta^1\text{-}NO_3)_2]$.[26]

(25) (a) Głwiak, T.; Kurdziel, K. *J. Mol. Struct.* **2000**, *516*, 1. (b) Carr, P.; Piggott, B.; Tinton, H. J. *Acta Crystallogr., Sect. C* **1985**, *41*, 372. (c) Turpeinen, E. *Suom. Kemistil. B* **1973**, *46*, 208. (d) Diamantopopoulou, E.; Zafiropoulos, T. F.; Perplepes, S. P.; Raptopoulou, C. P. Terzis. A. *Polyhedron* **1994**, *13*, 1593. (e) Claramunt, R. M; Domiano, P.; Elguero, J.; Lavandera, J. L. *Bull. Soc. Chim. Fr.* **1989**, 472.

Table 2. Bond Distances and Angles for Complexes **1**−**4**

	1	2		**3** (X = O11)	**4** (X = O2)
Ni−N11	2.027(2)	2.0284(16)	Ni−N11	2.0630(13)	2.0593(14)
Ni−N21	1.994(2)	2.0329(16)	Ni−N21	2.0841(14)	2.0806(14)
Ni−O1	2.080(2)	2.1293(15)	Ni−N31	2.0952(14)	2.0971(13)
Ni−O2	2.113(2)	2.1017(14)	Ni−N41	2.0567(14)	2.0686(13)
Ni−O4	2.081(2)	2.0591(16)	Ni−O1	2.0724(12)	2.1273(12)
Ni−O5	2.093(2)	−	Ni−X	2.1409(13)	2.0925(11)
N11−Ni−N21	89.61(9)	88.81(7)	N11−Ni−N21	86.81(5)	86.24(5)
N11−Ni−O1	105.89(9)	103.30(7)	N11−Ni−N31	96.65(5)	94.68(5)
N11−Ni−O2	167.40(9)	164.25(7)	N11−Ni−N41	101.37(5)	99.46(5)
N11−Ni−O4	97.83(9)	86.80(7)	N21−Ni−N31	175.00(5)	177.85(5)
N11−Ni−O5	93.28(9)	−	N21−Ni−N41	97.31(6)	95.03(5)
N21−Ni−O1	102.42(9)	94.06(6)	N31−Ni−N41	85.58(5)	86.74(5)
N21−Ni−O2	91.91(9)	90.45(6)	N11−Ni−O1	170.79(5)	173.67(5)
N21−Ni−O4	97.75(9)	91.00(7)	N11−Ni−X	81.83(5)	88.25(5)
N21−Ni−O5	159.56(9)	−	N21−Ni−O1	87.66(5)	90.95(5)
O1−Ni−O2	61.58(9)	61.06(6)	N21−Ni−X	87.17(6)	86.91(5)
O1−Ni−O4	148.73(9)	168.78(6)	N31−Ni−O1	88.44(5)	87.94(5)
O1−Ni−O5	96.23(9)	−	N31−Ni−X	89.73(6)	91.18(5)
O2−Ni−O4	94.35(10)	108.95(6)	N41−Ni−O1	86.63(5)	86.43(5)
O2−Ni−O5	89.65(9)	−	N41−Ni−X	174.59(6)	172.15(5)
O4−Ni−O5	61.81(8)	−	O1−Ni−X	90.55(5)	85.93(5)
Ni−N3	−	2.0650(18)	−	−	−
N11−Ni−N3	−	92.92(7)	−	−	−
N21−Ni−N3	−	178.21(7)	−	−	−
N3−Ni−O1	−	86.03(7)	−	−	−
N3−Ni−O2	−	88.03(7)	−	−	−
N3−Ni−O4	−	88.60(7)	−	−	−

A number of observations have indicated that all the ligands in **3** and **4** are fairly labile and can be displaced by coordinating solvents. Thus, the UV−vis−NIR spectra of **3** and **4** displayed small but significant variations as a function of solvent (vide infra), while their NMR spectra in CD_3CN led to a gradual broadening of the original peaks and gave rise to signals for free dpdpm (vide infra). Unfortunately, however, we were unable to intercept and isolate any solvato derivatives of **3** or **4**. In contrast, complex **1** reacted readily with water, MeOH or CH_3CN to give blue solvato derivatives, and we succeeded in isolating and characterizing the acetonitrile derivative [(dpdpm)Ni(η^2-NO_3)(η^1-NO_3)(CH_3CN)], **2** (vide infra).

Finally, we were unable to prepare the homoleptic complex $[Ni(dpdpm)_3][NO_3]_2$ from the reaction of excess dpdpm (>5 equiv) with $Ni(NO_3)_2$, **3**, or **4**, whereas reacting **1** with excess dpdpm gave **3** (Scheme 1). The precise reasons for our failure to prepare a tris(dpdpm) complex are not known, but we can rule out steric or enthalpic factors since we have observed the formation of $[Ni(dpdpm)_3]^{2+}$ from NiI_2.[27]

Crystal Structures. Single crystals of **1**, **2**, **3**, and **4** were obtained by vapor diffusion of Et_2O into solutions of these complexes in CH_2Cl_2, acetonitrile, methanol, and acetone, respectively. To ensure that the crystals retain their integrity throughout the data collection period, they were coated by either Paratone-N oil or epoxy glue and mounted rapidly. All four sets of diffraction data resulted in fairly accurate structures for the complexes studied, as reflected in the R_1 values of ca. 0.0444 (**1**), 0.0525 (**2**), 0.0506 (**3**), and 0.0325 (**4**). The crystal data and details of data collection are listed in Table 1, the principal geometric parameters are listed in Table 2, and ORTEP III[28] molecular structures are illustrated in Figures 1−4.

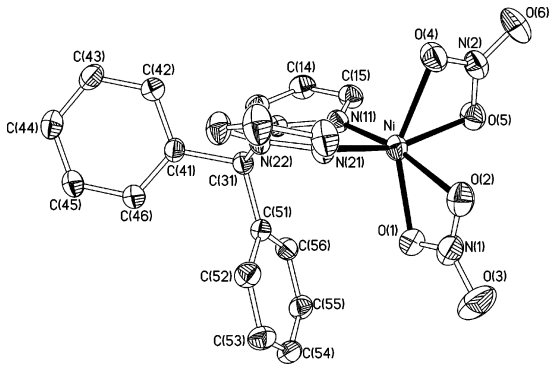

Figure 1. ORTEP view of complex **1**. Thermal ellipsoids are shown at 30% probability.

All four complexes adopt variously distorted octahedral structures. The small bite angle of the bidentate nitrate ligands causes the largest distortions from ideal octahedral geometry in complexes **1** and **2**: *cis*-O−Ni−O angles are ca. 62°, while *trans*-O−Ni−O and *trans*-O−Ni−N angles are ca. 149−167°. Further distortions are introduced by the significantly different Ni−O bond distances in **1** (Ni−O1∼Ni−O4 < Ni−O5 < Ni−O2) and **2** (Ni−O4 < Ni−O2 < Ni−O1). By comparison, the bis(dpdpm) species **3** and **4** show somewhat less pronounced angular distortions because

(26) Two structurally related mono(η^2-NO_3) compounds have been reported recently: $[(bpm^*)_2Ni(\eta^2\text{-}NO_3)][NO_3]$ (ref 10) and $[(pz_2thCH)_2Ni(\eta^2\text{-}NO_3)][NO_3]$ (pz_2thCH = bis(pyrazolyl)(2-thienyl)methane; Astley, T.; Hitchman, M. A.; Skelton, W. B.; White, A. H. *Aust. J. Chem.* **1997**, *50*, 145.)

(27) The preparation and full characterization of this compound and related species arising from the reaction of nickel halides will be the subject of an upcoming report.

(28) Burnett, M. N.; Johnson, C. K. (1996). ORTEPIII - Oak Ridge Thermal Ellipsoid Plot Program for Crystal Structure Illustrations, Technical Report ORNL-6895. Oak Ridge National Laboratory, TN.

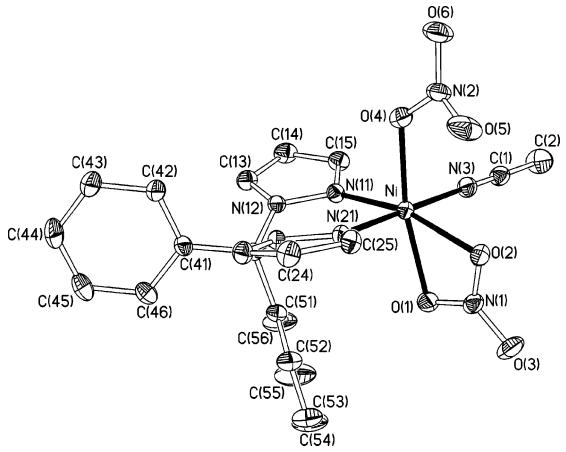

Figure 2. ORTEP view of complex **2**. Thermal ellipsoids are shown at 30% probability. Only one of the two positions (0.50:0.50) is shown for the disordered O5 atom. The disordered Et_2O molecule has been omitted for clarity.

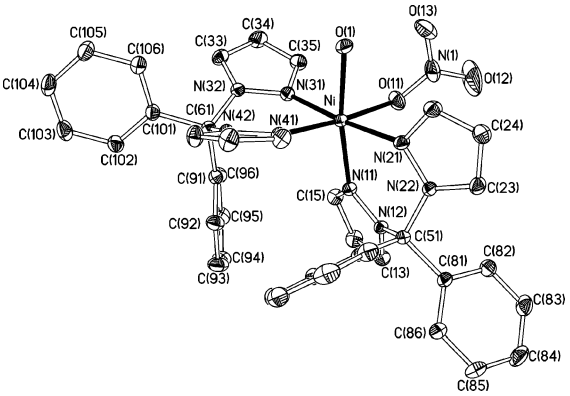

Figure 3. ORTEP view of complex **3**. Thermal ellipsoids are shown at 30% probability. The NO_3^- counterion has been omitted for clarity.

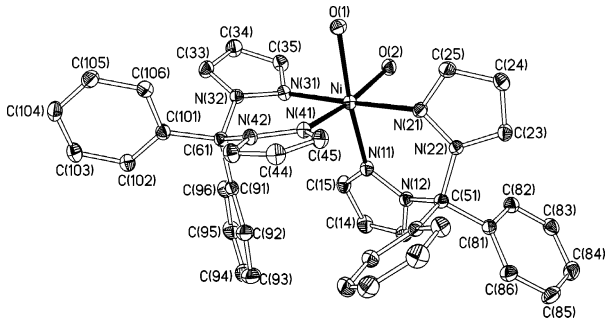

Figure 4. ORTEP view of complex **4**. Thermal ellipsoids are shown at 30% probability. The NO_3^- counter ions have been omitted for clarity.

of the absence of a chelating nitrate in these complexes and the fact that the two dpdpm ligands in these compounds adopt fairly regular *cis* and *trans* N-Ni-N angles (∼86−102° and 175−178°).

Inspection of the $Ni-O_{nitrate}$ distances in the structures of **1** and **2** supports our previously proposed[10] trans influence orders of pyrazolyl > η^2-O_2NO and η^1-ONO_2 > η^2-O_2NO. For instance, Ni−O1, Ni−O4 < Ni−O2, Ni−O5 in **1**, and Ni−O4 < Ni−O1 in **2**. In addition, the pyrazolyl ligand also appears to have a somewhat greater trans influence than η^1-NO_3 and water: Ni−N21, Ni−N31 > Ni−N11, Ni−N41 in **3**; Ni−N21, Ni−N31 > Ni−N11, Ni−N41 in **4**. On the other hand, since the difference between Ni−N11 and Ni−N41 in **3** is statistically insignificant ($\pm 3\sigma$), we conclude that water and η^1-NO_3 possess very similar trans influences. Finally, inspection of $Ni-N_{pyrazolyl}$ distances in the structure of **2** indicates that CH_3CN and η^2-NO_3 possess fairly similar trans influence values. Combining these observations gives the following trans influence order: pyrazolyl ∼ H_2O ∼ η^1-ONO_2 > NCMe ∼ η^2-O_2NO.

Magnetic and Spectroscopic Studies. Magnetic susceptibility measurements using the Gouy method have established that μ_{eff} for complexes **1**, **3**, and **4** are between 3.1 and 3.4 BM, whereas that of complex **2** is 3.9 BM. These magnetic susceptibilities are somewhat higher than the corresponding values obtained for our previously reported bis- and tris-(pyrazolyl)methane complexes of nickel (2.8−3.3 BM);[10] nevertheless, all of these values are in the expected range for octahedral Ni(II) complexes,[29] and they indicate the presence of two unpaired electrons.

The ^1H NMR spectra of these complexes display broad and, for the most part, featureless signals that serve primarily as fingerprints for identifying this family of complexes and provide little structural information. We believe that the broadness of the signals is caused primarily by the paramagnetism of the compounds, but this family of bis-(pyrazolyl)alkane ligands can also undergo a dynamic exchange process involving the flip of the M−N−N−C−N−N ring between chair and boat conformations. Moreover, in the NMR spectra of complexes **4** and **2** the ligand peaks appear to be somewhat broader when the spectra are run in CD_3CN. Since the peak due to residual solvent signal (CHD_2-CN) is also fairly broadened, we suspect that these observations are due to a ligand exchange process whereby solvent molecules displace dpdpm ligand from the coordination sphere of the complexes. It should be added, however, that no dpdpm-free complexes have been obtained in the solid state.

The IR spectra of the complexes show a large number of absorptions. The very strong signals observed at 1491 and 1278 cm^{-1} in the IR spectrum of **1** are tentatively attributed to the η^2-NO_3 moiety. For comparison, the corresponding absorptions in the analogous complex [(bpm*)$_2$Ni(η^2-NO_3)]-[NO_3] were found at 1480 and 1290 cm^{-1}.[10,30] The complexes bearing monodentate nitrate ligands give rise to sharp peaks at 1448−1438 and 1384 cm^{-1} (**3**) and at 1450−1435 and 1384 (**2**). Finally, the nitrate counter anions in **4** gave rise to absorptions at 1449−1385 and 1332−1306 cm^{-1}.

The different colors of the complexes under discussion (green for **1**, blue for **2**, **3**, and **4**) hinted at energetic differences in the electronic transitions for these d^8 complexes. Although Laporte rules stipulate that d−d transitions are forbidden in perfectly octahedral complexes, the geometrical distortions present in our compounds would be

(29) Collinson, S. R.; Schröder, M. Nickel: Inorganic and Coordination Chemistry. In *Encyclopedia of Inorganic Chemistry*, 2nd ed.; King, R. B., Ed.; Wiley InterScience: 2006; Vol. VI.

(30) For a general discussion of NO_3 stretching frequencies, see: Nakamoto, K. *Raman Spectra of Inorganic and Coordination Compounds. Part B: Applications in Coordination, Organometallic and Bioinorganic Chemistry*, 5th ed.; Wiley: 1997; Chapter 8, pp 87−88.

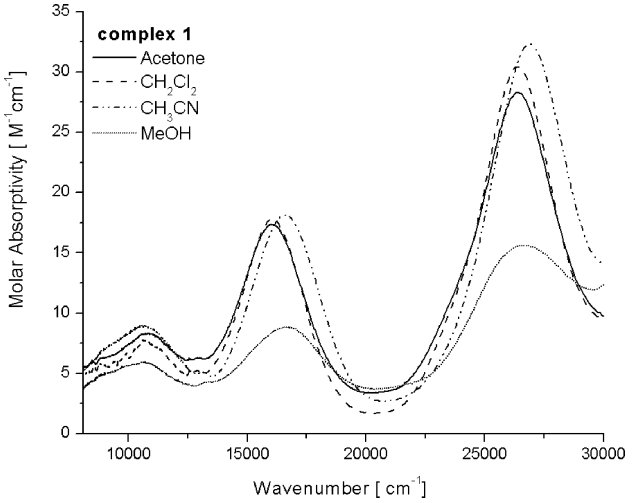

Figure 5. UV−vis−NIR spectra of complex **1** in different solvents.

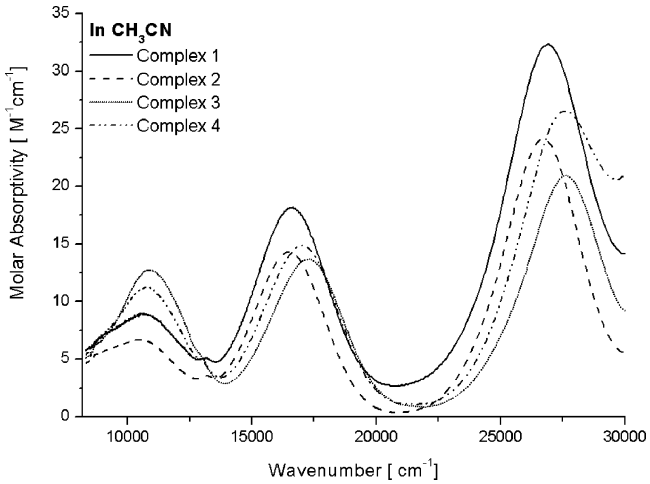

Figure 6. The UV−vis−NIR spectra of complexes **1**, **2**, **3**, and **4** in acetonitrile.

expected to facilitate weak d−d transitions. UV−vis spectroscopy was, therefore, used to delineate the differences in the electronic states of complexes **1**−**4**. Given the possibility of geometrical changes in solution upon solvent coordination, the UV−vis−NIR spectra were recorded in acetone, CH_2Cl_2, CH_3CN, and MeOH (Figure 5 for complex **1**, and Figures 5a−c in Supporting Information for complexes **2**−4).

As expected for octahedral d^8 complexes,[31] complexes **1**−**4** displayed three main bands featuring low molar absorptivities at around 1000, 650, and 380 nm; a weak shoulder was also detected at about 700−800 nm in most spectra.[32] Table 3 lists the band maxima and molar absorptivities for all four complexes. All bands have been assigned from the Tanabe−Sugano diagram for octahedral complexes, as follows. The three main bands represent spin allowed (d−d) transitions from the ground state $^3A_{2g}$ to the $^3T_{2g}$, $^3T_{1g}(^3F)$, and $^3T_{1g}(^3P)$ excited states commonly observed for essentially octahedral nickel(II) complexes. Weak features due to spin forbidden transitions $^3A_{2g} \rightarrow {}^1Eg$ also occur at energies intermediate between the $^3A_{2g} \rightarrow {}^3T_{2g}$ and $^3A_{2g} \rightarrow {}^3T_{1g}(^3F)$ transitions.[33] The observation of this spin-forbidden transition is thought to be facilitated by the close proximity of $^3A_{2g} \rightarrow {}^3T_{2g}$ and $^3A_{2g} \rightarrow {}^1Eg$ transitions, which leads to a strong mixing through spin−orbit coupling and an increase of the intensity and bandwidth for the spin-forbidden transition.[12]

Qualitative analysis of the electronic spectra for these complexes in different solvents allows us to speculate on possible solvent−Ni interactions. For instance, the transition energies are quite similar in the acetone and CH_2Cl_2 spectra, but fairly different in the MeOH spectra, especially in the case of complexes **3** and **4** (Figures 5b and 5c in Supporting Information); these observations hint at possible MeOH−Ni interactions in these complexes. As mentioned earlier, however, no MeOH adducts have been isolated in the solid, implying that the aquo adducts crystallize more readily. Moreover, the similarity of the spectra recorded for acetone and CH_2Cl_2 samples of **1** (Figure 5) and **2** (Figure 5a in Supporting Information) suggests that the coordinated CH_3CN in complex **2** likely dissociates in these solvents, thus forming **1**.

The well-resolved bands for the three main transitions have allowed us to determine the 10Dq value and Racha parameter, B, for each complex based on the following equations:[34]

$$10Dq = E(^3A_{2g} \rightarrow {}^3T_{2g}) = \nu 1 \quad (1)$$

$$15B = E(^3A_{2g} \rightarrow {}^3T_{1g}(^3F)) + E(^3A_{2g} \rightarrow {}^3T_{1g}(^3P)) - 3Dq = \nu 2 + \nu 3 - 3\nu 1 \quad (2)$$

All calculated values for 10Dq and B in various solvents are listed in Table 3. The 10Dq parameters (Δ) for **1**−**4** are remarkably similar for all four complexes (e.g., 10805−10870 cm^{-1} for spectra of acetone solutions). Interestingly, the largest 10Dq and B values are found in acetone spectra. In order to establish a possible correlation between structural features and crystal field parameters, we have compiled a list of these parameters for a range of octahedral Ni(II) complexes in Table 4. Comparison of this data reveals similarly uniform 10Dq values (within 500 cm^{-1}) for the analogous complexes of Ni bearing bpm^* and tpm^* ligands,[12] implying that within a family of closely related compounds the 10Dq value is fairly insensitive to structural variations such as the nature of ligator atoms (N:O ratio), the bonding mode of the nitrate ligand, and the overall charge. Indeed, the only complexes that give rise to significantly different 10Dq values are $[Ni(H_2O)_6]^{2+}$ and $[Ni(o\text{-phenanthroline})_3]^{2+}$. On the other hand, greater variations are observed in the

(31) Sacconi, L.; Mani, F.; Bencini, A. Nickel. In *Comprehensive Coordination Chemistry*; Wilkinson, G., Gilard, R., McCleverty, J., Eds.; Pergamon Press: Oxford, 1987; Vol. 5, p 58.

(32) Very similar "weak shoulders" have been observed in the absorption spectra of $[Ni(NH_3)_6]^{2+}$. For a discussion, see: Triest, M.; Bussière, G.; Bélisle, H.; Reber, C. *J. Chem. Educ.* **2000**, *77*, 670. Available at http://jchemed.chem.wisc.edu/jcewww/articles/JCENi/JCENi.html.

(33) For a description of this phenomenon, including detailed analyses of these transitions based on Tanabe-Sugano diagrams and modern theoretical models, see: Nolet, M.-C.; Beaulac, R.; Boulanger, A.-M.; Reber, C. *Struct. Bonding* **2004**, *107*, 145.

(34) (a) Reedijk, J.; Van Leeuwen, P. W. N. M.; Groeneveld, W. L. *Recl. Trav. Chim. Pays-Bas* **1968**, *87*, 129. (b) König, E. *Struct. Bonding* **1971**, *9*, 175.

Table 3. Absorption Energies, Molar Absorptivities, and Crystal Field Parameters for Spin-Allowed Bands of UV−Vis−NIR Spectra for Complexes **1**−**4** in Different Solvents[a]

		E (cm^{-1}), ϵ (M^{-1} cm^{-1})					
complex	solvent	$\nu1 = 10Dq$	Eg	$\nu2$	$\nu3$	B (cm^{-1})	10Dq/B
1	acetone	10784, 8	12946, 6	16043, 17	26395, 28	672	16.0
	CH_2Cl_2	10639, 8	12892, 5	16001, 18	26268, 30	690	15.4
	CH_3CN	10633, 9	13122, 5	16588, 18	26894, 32	772	13.8
	MeOH	10595, 6	13378, 4	16638, 9	26669, 16	767	13.8
2	acetone	10786, 8	12743, 6	16315, 12	26650, 18	707	15.2
	CH_2Cl_2	10685, 7	12781, 4	16075, 11	26593, 20	707	15.1
	CH_3CN	10537, 8	13205, 4	16483, 17	26706, 24	772	13.6
	MeOH	10391, 4	13360, 3	16531, 7	26355, 10	781	13.3
3	acetone	10835, 15	12817, 8	16605, 20	26986, 32	739	14.7
	CH_2Cl_2	10820, 13	−	16803, 14	27122, 32	764	14.1
	CH_3CN	10883, 13	13839, 3	17249, 14	27625, 21	815	13.4
	MeOH	10485, 7	12921, 3	16805, 9	26776, 13	808	12.97
4	acetone	10805, 11	13231, 6	16437, 18	26948, 33	731	14.8
	CH_2Cl_2	10779, 9	−	16643, 13	27097, 28	760	14.0
	CH_3CN	10744, 11	13989, 4	16998, 15	27610, 27	824	13.0
	MeOH	10614, 6	13280, 2	16770, 9	27210, 17	809	13.1

[a] The spectra were recorded at room temperature. 10Dq and B values were calculated from eqs 1 and 2 in the text.

Table 4. Crystal Field Parameters for **1**−**4** and Related Compounds

compound	N:O	10Dq (cm^{-1})	B (cm^{-1})	10Dq/B	ref
$[Ni(H_2O)_6]^{2+}$	0:6	8580	929	9.2	32
complex **1**	2:4	10633	772	13.8	this work
complex **2**	3:3	10537	772	13.6	this work
(tpm[a])Ni(η^2-NO_3)(η^1-NO_3)	3:3	10300	837	12.3	12
[(bpm[a])$_2$Ni(η^2-NO_3)]$^+$	4:2	10170	869	11.7	12
complex **3**	4:2	10883	815	13.4	this work
complex **4**	4:2	10744	824	13.0	this work
[(bpm[a])(tpm[a])Ni(η^1-NO_3)]$^+$	5:1	10420	891	11.7	12
$[Ni(tpm^a)_2]^{2+}$	6:0	11670	786	14.8	12
$[Ni(pyrazol)_6]^{2+}$	6:0	10650	843	12.6	36
$[Ni(NH_3)_6]^{2+}$	6:0	10730	830	12.9	32
[Ni(*o*-phenanthroline)$_3$]$^{2+}$	6:0	12690	710	17.9	33

[a] All spectra have been recorded for acetonitrile solutions.

Scheme 2

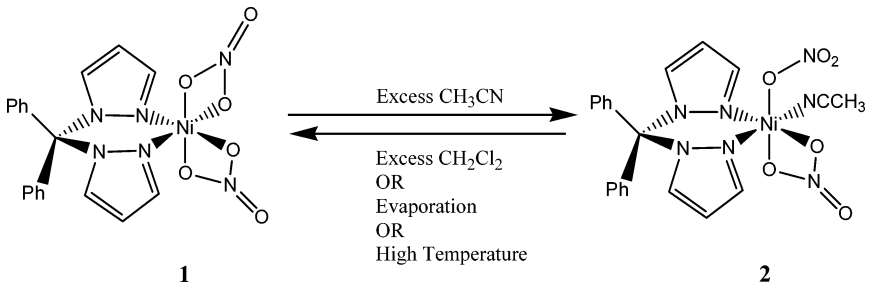

10Dq/B ratios for all the complexes (Table 4). Thus, the values of ca. 13−16 for complexes **1**−**4** are intermediate between the corresponding values reported for the homoleptic dicationic complexes $[NiL_6]^{2+}$ bearing strong-field ligands such as *o*-phenanthroline (17.9)[33] and weak-field ligands such as water (9.2).[35] Nevertheless, there appears to be no simple correlation between the 10Dq/B ratio and the structural parameters.

Solvato-, Vapo-, and Thermochromic Properties of Complexes 1 and 2. As mentioned earlier, dissolving **1** (green) in CH_3CN gave a blue species that was identified as the CH_3CN adduct **2** arising from the $\eta^2 \rightarrow \eta^1$ hapticity change of a nitrate ligand. A series of experiments established that the interconversion of **1** and **2** is reversible (Scheme 2). Thus, evaporation of blue solutions obtained by dissolving **1** in CH_3CN gave back green samples of **1**, which produced blue solutions when redissolved in CH_3CN. This process could be repeated several times. UV−vis spectroscopy showed that the presence of greater proportions of CH_3CN in CH_2Cl_2 solutions of **1** resulted in an incremental blue-shift in the high-energy band maximum, from ca. 381 nm for **1** (100% CH_2Cl_2) to ca. 374 nm for **2** (80% CH_3CN), as shown in Figure 7. Similar green-to-blue color changes were noted in CH_2Cl_2/MeOH and acetone/water mixtures, but the new species arising from the interaction of MeOH and water with the Ni center in **1** have not been identified.

(35) Bussière, G.; Reber, C. *J. Am. Chem. Soc.* **1998**, *120*, 6306.

(36) Reimann, C. W. *J. Phys. Chem.* **1970**, *74*, 561.

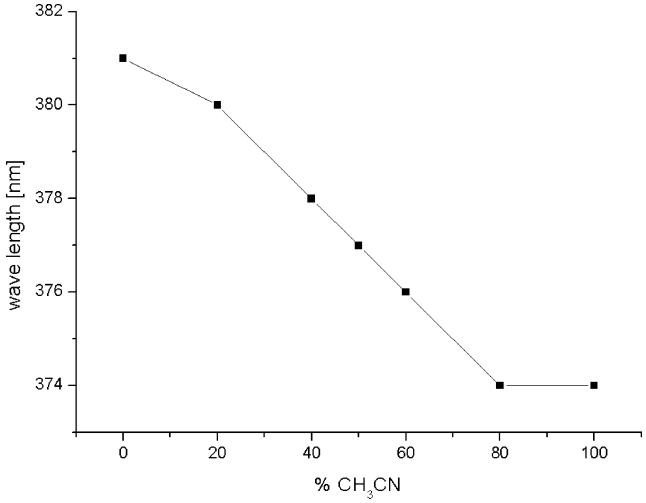

Figure 7. Shift in the absorption wavelength of the high-energy band in the UV−visible spectra of **1** as a function of solvent composition (CH_2Cl_2:CH_3CN).

The temperature-dependence of the CH_3CN-induced $\eta^2 \rightarrow \eta^1$ hapticity change of one of the nitrate ligands in **1** was studied briefly, as follows. The blue solution obtained by dissolving a sample of **1** in CH_3CN was heated gradually to ca. 80 °C and its color was monitored. A gradual, blue-to-green color change was observed up to ca. 65 °C, at which point the green color was dominant. Further heating to ca. 80 °C only deepened the green color, whereas allowing the solution to cool to room temperature re-established the original blue color. Repeating this heating/cooling cycle 10 times showed that the heat-induced interconversion of **1** and **2** was reversible. On the other hand, variable temperature UV−vis spectra of a CH_3CN solution of **1** confirmed that complexes **1** and **2** are in equilibrium, the major species being complex **2** below 0 °C (band maximum for ν_3 at 372 nm) and complex **1** above 70 °C (band maximum for ν_3 at 378 nm).

That this CH_3CN-induced $\eta^2 \rightarrow \eta^1$ slippage of one of the nitrate ligands in **1** can take place in solutions raised the question of whether or not this process might take place by exposure of solid samples to CH_3CN vapor. Tests showed that green samples of **1** turned blue when exposed to CH_3CN vapor, while the resulting blue solid (or independently prepared samples of **2**) turned green when heated briefly (1−2 min at ca. 100 °C) or placed under vacuum. This reversible interconversion of **1** and **2** took place over several cycles without degradation.

Conclusion

The preparation and characterization of complexes **1**−**4** has allowed us to study the structural and spectroscopic properties of a new series of Ni(II) complexes bearing the dpdpm ligand. The solid state structures of these complexes are fairly similar to those of the analogous bpm* complexes reported earlier,[10] implying that the different sterics of these two ligands have little or no influence over the structures adopted by their complexes. These closely related complexes also display fairly comparable UV−vis−NIR spectra, implying that the electronic structures of this family of complexes are not very sensitive to subtle structural differences.

The most intriguing aspect of the present study is the solvato-, thermo-, and vapochromism of complex **1**, which is caused by the reversible coordination of acetonitrile to the Ni center in **1** and the resulting conversion of one of the η^2-NO_3 to η^1-NO_3. That the formation of complex **1** is favored at higher temperature is presumably due to entropic factors that tend to favor the chelation of the nitrate ligand and the dissociation of a molecule of acetonitrile. Future investigations will probe the vapo- and thermochromic properties of thin films produced from polymer matrices containing complex **1**.

Acknowledgment. The Natural Sciences and Engineering Research Council of Canada and Fonds Québécois de la Recherche sur la Nature et les Technologies are gratefully acknowledged for their financial support. We are grateful to Profs. G. Hanan and C. Reber and their research groups for their valuable help with the UV−vis−NIR spectra.

Supporting Information Available: UV−vis spectra of complexes **2**−**4** in different solvents (Figures 5a−c). This material is available free of charge via the Internet at http://pubs.acs.org. Crystallographic data for the structural analysis have been deposited with the Cambridge Crystallographic Data Centre, CCDC No. 614549 (**1**), 614551 (**2**), 614552 (**3**), 614550 (**4**). Copies of this information may be obtained free of charge from The Director, CCDC, 12 Union Road, Cambridge CB2 1EZ, U.K. (Fax: +44-1223-336-033. E-mail: deposit@ccdc.cam.ac.uk or www: http://www.ccdc.cam.ac.uk).

IC061311Z